Reprinted from:

THE JOURNAL OF CHEMICAL PHYSICS VOLUME 59, NUMBER 5 1 SEPTEMBER 1973

Microwave optical double resonance spectroscopy with a cw dye laser: BaO $X\,^1\Sigma$ and $A\,^1\Sigma$*

Robert W. Field, Alan D. English, Takehiko Tanaka†, David O. Harris, and Donald A. Jennings‡

Quantum Institute, University of California, Santa Barbara, California 93106

(Received 23 May 1973)

A tunable, single frequency, continuous wave, dye laser has been used to optically pump various lines of the BaO $A\,^1\Sigma$–$X\,^1\Sigma$ electronic transition. Microwave optical double resonance (MODR) spectra are recorded as changes in the intensity of dye laser induced photoluminescence. Fourteen microwave rotational transitions in the $X\,^1\Sigma$ ($v = 0,1$) and $A\,^1\Sigma$ ($v = 0$–5) states of $^{138}Ba^{16}O$ and one transition in the $A\,^1\Sigma$ ($v = 1$) state of $^{137}Ba^{16}O$ have been observed. Partially deperturbed rotational constants obtained for BaO $A\,^1\Sigma$ are $B(v) = 0.25832(2) - 0.001070(5)\,(v + 1/2)$ cm^{-1}. Two physical models are described which account for microwave optical double resonance effects in the strong (nonlinear) and weak (linear) optical pumping limits. Observed changes in photoluminescence polarization caused by excited state microwave transitions are predicted by a semiclassical transition dipole model. A three level steady state kinetic treatment of microwave optical double resonance indicates that the BaO MODR transitions reported in this paper are observed near the strong optical pumping limit. It is shown that for most allowed transitions in diatomic molecules a 100 mW single frequency, dye laser is sufficiently intense to significantly deplete rotational levels of the electronic ground state with respect to neighboring rotational levels and to cause the populations of the depleted ground state and optically pumped excited state levels to become comparable.

I. INTRODUCTION

A tunable, continuous wave, dye laser has been used to obtain microwave optical double resonance (MODR) spectra of BaO. In a MODR experiment, a single molecule absorbs (or is stimulated to emit) two photons: one microwave and one optical (ir, visible, uv). Resonant absorption of one type of photon is detected as a change in the absorption or emission of the other type of photon. In the MODR experiments reported here, microwave transitions are observed between adjacent rotational levels in several vibrational levels of the BaO $X\,^1\Sigma$ and $A\,^1\Sigma$ electronic states. Microwave transitions are detected optically as a change in the intensity of rotationally unresolved photoluminescence. These experiments establish the possibility of observing microwave spectra in vibrationally and electronically excited states of the large class of molecules which will absorb light within the tuning range of extant cw dye lasers.

Microwave optical double resonance experiments have been reported previously using incoherent[1,2,3] and laser[4,5,6,7] optical pumps. Both pulsed[8,9] and cw[10] dye lasers have been used for high resolution spectroscopy, but no double resonance experiments have been reported using dye lasers. Optical pumping effects in molecules in which a laser aligns a ground state rotational level by preferentially depleting certain magnetic sublevels $|M|$ have been described by Drullinger and Zare.[11] MODR experiments reported here are near the strong optical pumping limit in which the population of one ground state rotational level is significantly depleted with respect to adjacent rotational levels and in which the population of the optically pumped excited level is at least 1% of the population of the optically depleted level of the ground state.

The purpose of this paper is threefold: first, to expose the physical basis for the observability of MODR, second, to describe the first successful use of a dye laser in a double resonance experiment, and, third, to present results of MODR experiments on BaO which validate the physical models given and which exemplify the precision, quantity, and significance of MODR spectroscopic measurements. A combination of two physical models accounts for MODR effects observed with BaO. Most of the MODR signal is explained by a three level steady state kinetic treatment of MODR near the strong optical pumping limit. In addition, clearly observable polarization dependent effects in excited state MODR are explained by a semiclassical transition dipole model. An important feature of the transition dipole model is that large excited state MODR effects in the weak optical pumping limit are predicted. It also will be shown that it is reasonable to expect, even for molecular transitions where the excited state has a considerably shorter radiative lifetime than BaO $A\,^1\Sigma$ (300 nsec), that it will be possible to achieve the strong optical pumping limit with available cw dye lasers.

The BaO $A\,^1\Sigma$ state is known to be perturbed[12,13] and these perturbations are evident in the rotational constants we report. It has been possible to adjust the $A\,^1\Sigma$ rotational constants to compensate for the effects of the largest perturbations. One

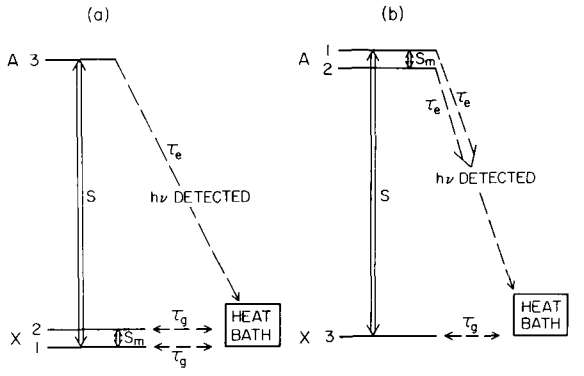

FIG. 1. Three level system corresponding to ground state [1(a)] and excited state [1(b)] MODR. S and S_m are, respectively, the laser and microwave transition rate constants. Only levels of the lower electronic state (X) are in equilibrium with the heat bath and have a relaxation time τ_g. The upper state levels (A) radiate with radiative lifetime τ_e. It is assumed that when the upper states spontaneously emit a photon, $h\nu$, the molecule enters the heat bath rather than returning to the optically-depleted ground state level.

of the important future applications of MODR spectroscopy will be the detailed analysis of interactions between electronically excited states.

II. DISCUSSION

MODR experiments on BaO belong to a general class of experiments in which the occurrence of a microwave transition is detected optically. A change in the intensity, polarization, or wavelength of emitted optical radiation occurs as a result of resonant absorption of microwave radiation. In previously reported related optical detection experiments, the emitting levels have been populated chemically,[14] by electron bombardment (MOMRIE),[15] indirectly by optical pumping followed by intersystem crossing (PMDR, ODMR, and optically detected ENDOR),[16] and by direct optical pumping (ORFDR[1-3] and MODR).[6,7] The proliferation of acronyms should not obscure the close similarity of various experimental techniques. In each, absorption of a microwave photon with energy much less than kT (at 300 °K) is observed by detection of an emitted optical photon of energy much greater than kT. Direct optical pumping MODR experiments may be divided into two limiting types: weak (linear absorption)[1-3] and strong (nonlinear absorption)[6,7] optical pumping.

In linear optical pumping experiments, the intensity of photoluminescence is linearly proportional to optical pump power, the population of the initial level is unaffected by optical pumping, and the population of the excited (pumped) level is insignificant (< 0.1%) with respect to the initial level. With a weak (linear) optical pump, a ground state microwave transition is detectable if microwave transitions alter the small Boltzmann population inequality between rotational levels; an excited state microwave transition is detectable if with some specific detection geometry and polarization or sufficient optical spectral resolution, the light emitted from one of the two excited state rotational levels connected by the microwave transition is preferentially detected. Although microwave transitions between rotational levels of electronic ground and excited states will be shown below to be detectable in the weak optical pumping limit, in the experiments reported here and particularly for MODR transitions in electronic ground states, strong optical pumping effects are larger and are easily attainable with dye laser optical pumps.

A. Linear Optical Pumping Steady State Effects

In the linear optical pumping limit, the population of the initial level of the optical transition [level 1 of Fig. 1(a)] is not affected by the presence of optical pump radiation. The steady state rate of production of emission from excited molecules [level 3 of Fig. 1(a)] is $(n_1 - n_3)S$. S is the optical transition rate constant and is proportional to laser power and n_1 and n_3 are populations of levels 1 and 3, respectively. Since $n_3 \ll n_1$, photoluminescence intensity is proportional to $n_1 S$. If the microwave transition between levels 1 and 2 is saturated, then

$$n_1 = (n_1^0 + n_2^0)/2 = n_1^0 + (n_2^0 - n_1^0)/2, \tag{1}$$

where n_1^0 and n_2^0 are thermal equilibrium populations of ground state levels 1 and 2 with energies E_1 and E_2. Thus the fractional change in n_1 at microwave resonance is

$$(n_1^0 - n_1)/n_1^0 \cong (E_1 - E_2)/2kT. \tag{2}$$

For example, for the $J'' = 2 \rightarrow 1$ transition of BaO at 300 °K, n_1 would change by 0.2%.

Figure 1(b) is the level diagram for excited state MODR effects. Note that the levels are labelled differently than in Fig. 1(a). Levels are numbered so that microwave transitions are always between levels 1 and 2 and optical transitions are always between levels 1 and 3. In excited state MODR [Fig. 1(b)] the ground state is level 3. Microwave transitions between the excited levels 1 and 2 are observable in the linear optical pumping limit, but not because the optical pumping rate $(n_3 - n_1)S$ changes. A saturated microwave transition alters n_1 by dividing excited molecules equally between levels 1 and 2. A change in n_1 results in an unobservably small change in the optical pumping rate because $n_1 \ll n_3$. Excited state MODR is observable in the weak pumping limit because light emitted from level 1 is polarized

differently than light emitted from level 2 (as shown in Sec. II. B). Light emitted from level 1 also has a slightly different wavelength than light emitted from level 2. At microwave resonance when excited molecules are transferred from level 1 to level 2, emission is transferred from level 1 to 2, but the total number of photons/sec emitted is unchanged. By taking advantage of either the difference between levels 1 and 2 in emission polarization or wavelength, the microwave induced transfer of emission from level 1 to 2 is observable.

B. Linear Optical Pumping Polarization Effects

Excited state MODR polarization effects in the linear optical pumping limit will be described with a semiclassical optical transition dipole model. One wishes to know the time-averaged squared projection of the molecular transition moment along the laboratory fixed Z axis $\langle \mu_Z^2 \rangle$. The radiation pattern from a dipole has a line of nodes along the dipole axis, is most intense in the plane normal to the dipole axis, and is linearly polarized parallel to the dipole axis. $\langle \mu_Z^2 \rangle$ is proportional to the fraction of molecular fluorescence emitted with Z polarization (and which propagates in the XY plane). It will be shown how microwave transitions with $\Delta J = \pm 1$ and $\Delta M = 0$ change $\langle \mu_Z^2 \rangle$.

Microwave transitions have the effect of changing the orientation of the molecular transition dipole with respect to the laboratory Z axis. A microwave induced change in $\langle \mu_Z^2 \rangle$, $\Delta\langle \mu_Z^2 \rangle$, results in compensating changes in the projection of the transition dipole on other laboratory axes

$$\Delta\langle \mu_Z^2 \rangle = -\Delta\langle \mu_X^2 \rangle - \Delta\langle \mu_Y^2 \rangle . \tag{3}$$

There is no net change in $\langle \mu^2 \rangle$. In the transition dipole model, the total number of photons/sec radiated is unaffected by microwave transitions.

The transition moment for a $^1\Sigma - ^1\Sigma$ transition in a diatomic molecule is located along the molecular axis. In a $^1\Sigma$ molecule the angular momentum vector **J** is perpendicular to the molecular axis. The projection of **J** on the space-fixed Z axis is M and the angle θ between **J** and Z is defined by

$$\cos\theta = M/[J(J+1)]^{1/2} . \tag{4}$$

Let ϕ be the angle (see Fig. 2) of rotation about **J** by which μ is rotated out of the plane defined by Z and **J**. The projection of μ on Z is then

$$\mu_Z = \mu \cos[(\pi/2) - \theta]\cos\phi, \tag{5}$$

$$\phi = \Omega t,$$

where Ω is the molecular rotational frequency in rad/sec. Since the rotational period is short with respect to a radiative lifetime, it is appropriate to

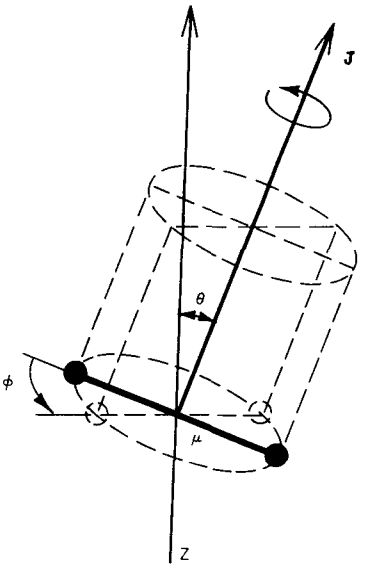

FIG. 2. Projection of transition dipole on laboratory fixed Z axis. θ is the angle separating J and Z. J and μ are orthogonal. J and Z lie in the plane of the paper. ϕ is the angle of rotation about J by which μ is lifted out of the plane of the paper.

average over ϕ:

$$\langle \mu_Z^2(\theta) \rangle = (1/2\pi) \int_0^{2\pi} \mu^2 \sin^2\theta \cos^2\phi \, d\phi, \tag{6}$$

$$\langle \mu_Z^2(M) \rangle = \tfrac{1}{2} \mu^2 \{1 - [M^2/J(J+1)]\} . \tag{7}$$

If the molecules are excited into some distribution of M levels $f(M)$ such that $\sum_{M=-J}^{J} f(M) = 1$, then

$$\langle \mu_Z^2 \rangle = \frac{\mu^2}{2} \sum_{M=-J}^{J} f(M)\{1 - [M^2/J(J+1)]\} . \tag{8}$$

This summation over M is equivalent to averaging over all orientations of **J** with respect to the space-fixed Z axis. Suppose, for simplicity, that the excited molecules are subjected to a microwave field with the E vector parallel to Z and which is so intense that $(J, M) \rightarrow (J+1, M)$ transitions are saturated for each M. Thus, with equal populations of levels (J, M) and $(J+1, M)$,

$$\langle \mu_Z^2 \rangle_{\text{Microwave}} = \frac{\mu^2}{2} \sum_{M=-J}^{+J} f(M) \left[1 - \frac{1}{2} \frac{M^2}{J(J+1)} - \frac{1}{2} \frac{M^2}{(J+1)(J+2)} \right] = \frac{\mu^2}{2} \sum_M f(M) \left[1 - \frac{M^2}{J(J+2)} \right], \tag{9}$$

$$\Delta\langle \mu_Z^2 \rangle \equiv \langle \mu_Z^2 \rangle_{\text{Microwave}} - \langle \mu_Z^2 \rangle = \frac{\mu^2}{2} \sum_M f(M) \times \left[\frac{M^2}{J(J+1)} - \frac{M^2}{J(J+2)} \right] = \frac{\mu^2}{2} \sum_M f(M) \frac{M^2}{J(J+1)(J+2)} . \tag{10}$$

Thus for $J \rightarrow J+1$, $\langle \mu_Z^2 \rangle$ will increase. This means that, at microwave resonance, emission propagating in the XY plane will increase in intensity at the expense of emission propagating in the Z direction and that Z polarized emission will increase in intensity. For $J \rightarrow J-1$ the resonant changes will be opposite in sign. It is clear that $f(M)$, which is determined by the intensity and polarization of the optical pumping radiation, can have no qualitative effect on the above conclusions. However, since this double resonance effect is proportional to M^2, an optical pumping scheme which favors the highest $|M|$ levels will maximize the double resonance effect. If optical pump radiation is X or Y polarized, high $|M|$ levels will be favored and the double resonance effect will be maximized.

If we let $f(M) = (2J+1)^{-1}$, then the fractional change at microwave resonance is

$$\Delta\langle \mu_Z^2 \rangle / \langle \mu_Z^2 \rangle = \sum_M M^2 [J+2]^{-1} \Big/ \sum_M [J(J+1) - M^2]$$

$$= 1/[2(J+2)]. \qquad (11)$$

If a $J' = 2 \rightarrow 3$ microwave transition is saturated, a 12% increase in emission polarized in the Z direction (parallel to the microwave electric field) is expected. Emission propagating in the X or Y direction is expected to increase by about 6% (corresponding to a 12% increase in Z-polarized radiation and a 6% decrease in Y- and X-polarized radiation).

C. Nonlinear Optical Pumping Steady State Effects

In nonlinear optical pumping experiments the total emission rate changes at microwave resonance because optical pumping has significantly depleted the initial (ground state) level and has caused the pumped (excited state) level to have a population comparable to the initial level. At microwave resonance the rate of production of excited molecules increases regardless of whether resonant microwave radiation induces a transition connected to the initial [level 1 of Fig. 1(a)] or final level [level 1 of Fig. 1(b)] of the optically pumped transition. The rate of production of excited state molecules $|n_1 - n_3| S$ increases at microwave resonance because ground state microwave transitions increase the steady state population of the optically-depleted level or because excited state microwave transitions decrease the steady state population of the optically-pumped level.

Strong optical pumping MODR effects may be understood from a steady state rate equation approach similar to that used by Takami and Shimoda.[17] One assumes that the rotational levels of the lower state are in equilibrium with a heat bath and have a characteristic relaxation time τ_g and that the excited state levels relax by spontaneous emission with a relaxation time τ_e. The (velocity dependent) optical transition rate constant S and the (velocity independent) microwave transition rate constant S_m are

$$S = (X^2/2)(\tau/\{1 + [\omega(1 - v/c) - \omega_{31}]^2 \tau^2\}), \qquad (12)$$

$$S_m = (X_m^2/2)(\tau_m/\{1 + (\omega_m - \omega_{21})^2 \tau_m^2\}), \qquad (13)$$

where

$$X = |\mu_{31}| E/\hbar, \qquad (14)$$

$$X_m = |\mu_{21}| E_m/\hbar, \qquad (15)$$

$\tau \approx \tau_e$,

$\tau_m \approx \tau_g$ [for ground state double resonance, Fig. 1(a)],

$\tau_m \approx \tau_e$ [for excited state double resonance, Fig. 1(b)],

μ is the electric dipole moment matrix element, $2E$ and $2E_m$ are the peak to peak electric field strengths of the optical and microwave fields, v is the component of velocity in the propagation direction of the laser, ω and ω_m are the angular frequencies of the laser and microwave radiation, and ω_{31} and ω_{21} are the angular frequencies corresponding to molecular energy level separations.

1. Ground State MODR

The rate equations which correspond to Fig. 1(a) (ground state microwave transition) are

$$dn_1/dt = S(n_3 - n_1) + S_m(n_2 - n_1) + (n_1^0 - n_1)/\tau_g, \qquad (16a)$$

$$dn_2/dt = S_m(n_1 - n_2) + (n_2^0 - n_2)/\tau_g, \qquad (16b)$$

$$dn_3/dt = S(n_1 - n_3) - (n_3/\tau_e). \qquad (16c)$$

n_i is the population per unit velocity of the ith level (with velocity v) and n_i^0 is the value of n_i in the absence of both radiation fields. The photoluminescence intensity is proportional to the total population of level 3, integrated over all velocities:

$$N_3 = \frac{\pi^{1/2} X^2 \tau_g}{2\omega(u/c)} \exp\left[-\left(\frac{\omega - \omega_{31}}{\omega u/c}\right)^2\right] \frac{N_1^0 + (N_1^0 + N_2^0) S_m \tau_g}{2 S_m \tau_g + 1}$$

$$\times \left[1 + \tau X^2 \frac{S_m \tau_g (\tau_g + 2\tau_e) + \tau_g + \tau_e}{4 S_m \tau_g + 2}\right]^{-1/2}, \qquad (17)$$

where $u = [2kT/M]^{1/2}$. In the strong microwave limit ($S_m \tau_g \gg 1$), the ratio of the photoluminescence intensity with microwaves on resonance to the intensity with microwaves off is

$$I(on)/I(off) \cong \{[1 + \tfrac{1}{2}(\tau_g + \tau_e)\tau X^2]/[1 + \tfrac{1}{4}(\tau_g + 2\tau_e)\tau X^2]\}^{1/2}. \qquad (18)$$

In the strong optical pumping limit ($\tau_g \tau X^2 \gg 1$), the value of the fractional change in photoluminescence at resonance is

$$\Delta I/I \equiv [I(on) - I(off)]/I(off) \tag{19}$$

$$\Delta I/I \to +40\% \quad \text{if } \tau_e \ll \tau_g \tag{20a}$$

$$\Delta I/I \to +15\% \quad \text{if } \tau_e = \tau_g . \tag{20b}$$

As the microwave power is decreased, the high optical power limiting values of $\Delta I/I$ decrease, and the limiting value is reached at about the same laser power ($1/2\tau_g \tau X^2 \approx 1$). $\Delta I/I$ saturates at considerably lower laser power than the photoluminescence intensity I. At the high optical power limit

$$\Delta I/I \cong \{[1 + 2S_m\tau_g]/ [1 + (\tau_g + 2\tau_e)(\tau_g + \tau_e)^{-1} S_m \tau_g]\}^{1/2} - 1. \tag{21}$$

In this limit $\Delta I/I$ increases approximately linearly with microwave power until $S_m\tau_g \approx 1$ at which point saturation occurs.

2. Excited State MODR

The rate equations which correspond to Fig. 1(b) (excited state microwave transition) are

$$dn_1/dt = S(n_3 - n_1) + S_m(n_2 - n_1) - (n_1/\tau_e), \tag{22a}$$

$$dn_2/dt = S_m(n_1 - n_2) - (n_2/\tau_e), \tag{22b}$$

$$dn_3/dt = S(n_1 - n_3) + (n_3^0 - n_3)/\tau_g . \tag{22c}$$

Level 1 is populated directly by optical pumping while level 2 is populated only by microwave induced transitions from level 1. Photoluminescence intensity is proportional to the sum of the total populations of levels 1 and 2. It was shown in Sec. II. B that photoluminescence from levels 1 and 2 will have different polarizations. For many detection geometries, including some in which linear polarizers are *not* included, different fractions of the photons emitted from levels 1 and 2 will strike the detector. The change in detected photoluminescence caused by excited state microwave transitions is

$$\Delta I/I = [N_1 + \alpha N_2 - N_1(S_m = 0)]/N_1(S_m = 0). \tag{23}$$

$N_1(S_m = 0)$ is the population of level 1 in the absence of microwave radiation and N_1 and N_2 are populations in the presence of microwave radiation with angular frequency $\omega_m = \omega_{12}$. α is the fraction of light striking the detector emitted from level 2 divided by the corresponding fraction of light emitted from level 1. For example, $\alpha = 0$ if rotationally-resolved photoluminescence originating exclusively from level 1 is monitored. In rotationally-unresolved experiments α is *approximately* but not *exactly* 1.

In the strong microwave limit ($S_m\tau_e \gg 1$)

$$\Delta I/I \cong [(1 + \alpha)/2]\{[1 + \tfrac{1}{2}(\tau_e + \tau_g)\tau X^2]/ [1 + \tfrac{1}{4}(\tau_e + 2\tau_g)\tau X^2]\}^{1/2} - 1. \tag{24}$$

As in ground state MODR, $\Delta I/I$ saturates at much lower laser power than I. If $\tau_e \ll \tau_g$, at the strong optical limit ($\tau_e \tau X^2 \gg 1$)

$$\Delta I/I \to (\alpha - 1)/2 . \tag{25a}$$

Note that in the unusual case when $\alpha = 1$ there is no double resonance effect. If $\tau_e = \tau_g$, then

$$\Delta I/I \to (3)^{-1/2}(1 + \alpha) - 1. \tag{25b}$$

In the strong optical limit

$$\Delta I/I \cong [1 + (1 + \alpha)\tau_e S_m]/\{(1 + 2\tau_e S_m)[1 + (\tau_e + 2\tau_g) \times (\tau_e + \tau_g)^{-1} S_m \tau_e]\}^{1/2} - 1 \tag{26}$$

and if $\tau_e \ll \tau_g$, then

$$\Delta I/I \cong (\alpha - 1)\tau_e S_m/(1 + 2\tau_e S_m). \tag{27}$$

Excited state MODR always disappears at the strong optical limit when $\alpha = 1$ and $\tau_e \ll \tau_g$ because rotational relaxation in the ground state cannot keep up with optical depletion of the ground state. The rate at which the laser pumps molecules out of level 3 can be no larger than the rate at which level 3 is collisionally repopulated. Ground state repopulation rates are unaffected by excited state microwave transitions.

III. EXPERIMENTAL

A. A cw Dye Laser as a MODR Optical Pumping Source

Microwave optical double resonance spectroscopy requires a light source for optical pumping which meets several requirements. It must have output at the wavelength of a molecular absorption line and it should be reproducibly and systematically tunable to preselected wavelengths. Frequency stability should be sufficient to remain within the Doppler width (± 150 MHz) of an absorption line for times as long as 1 h. Amplitude stability better than ± 20% is desirable. Sufficient optical pump power (> 20 mW) to cause the optically-pumped excited level to become comparable in population to the optically-depleted absorbing level is useful, but not absolutely necessary. Wavelength tunability is important to allow optical pumping experiments on a variety of rotational, vibrational, and electronic states of several molecules.

A cw rhodamine 6 G dye laser has been constructed after the design of Dienes *et al.*[18] as shown in Fig. 3. Astigmatic compensation, described by Kogelnik *et al.*[19] is used. A 514.5 nm Ar^+ laser with maximum power output of 2.5 W excites the dye laser. Selection of a steering mirror for the Ar^+ laser with 6 m radius of curvature (M_4 of Fig. 3) mode matches the Ar^+ and dye lasers within the dye cell. An aqueous dye solution with 3% detergent by volume flows at 10 m/sec through a 1 mm thick dye cell oriented at Brewster's angle. Dye concentration is adjusted for maximum dye

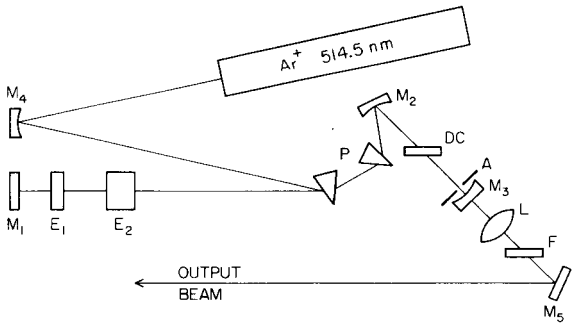

FIG. 3. cw dye laser single frequency configuration. M_1–M_5 are dielectric mirrors (radius of curvature, reflectivity) as follows: M_1 (∞, 100%), M_2 (10 cm, 100%), M_3 (5 cm, 94% at 580 nm), M_4 (6m, 100%), M_5 (∞, 100%). The dye cell is DC. E_1 and E_2 are solid etalons (flat $\lambda/10$, wedge < 0.5 sec). E_1 is 1.5 mm thick, with 30% reflectivity both sides. E_2 is 15 mm thick, with 20% reflectivity both sides. L is a 15 cm focal length antireflection-coated lens, P is a SF4 glass prism, F is a short wavelength cutoff filter (to exclude transmitted 514.5 nm radiation), and A is a 2.5 mm aperture. The end mirrors of the dye laser resonator M_1 and M_3 are separated by 190 cm. For clarity, the region of the dye cell is shown expanded.

laser power output in the wavelength region of interest.

Coarse wavelength tuning of the dye laser is accomplished without altering the position of the output beam, by rotating the return mirror (M_1 of Fig. 3) in the dispersion plane. The dispersive element in the cavity is two prisms. A lens is used to bring the strongly divergent output of the dye laser to a focus at the photoluminescence viewing region.

The dye laser operates from 563.5 to 629.0 nm with output power from 10 to 400 mW, but with frequency stability insufficient for our experiment. Frequency stability is improved when a 2.5 mm aperture is inserted in the cavity at the output mirror (M_3 of Fig. 3) to obtain spatial mode stability. In this configuration, the spectral bandwidth over which the laser has sufficient gain to lase is 100 GHz. However, the spectral bandwidth of the laser output is 10–15 GHz.

Additional frequency stability is obtained with intracavity etalons.[20] Optimum etalon free spectral range (FSR) is determined by cavity geometry, wavelength, and most importantly by the spectral bandwidth over which the laser has sufficient gain to lase (not the bandwidth over which the laser actually lases). Etalon reflectivity is selected for sufficient finesse, yet also to allow tuning of the etalon through at least one free spectral range without resulting in intolerable single pass intracavity losses (< 5%). A 1.5 mm thick solid etalon (FSR 70 GHz) with 30% reflectivity on each side is used. The resulting output of the laser is in two modes each with stability of ± 100 MHz and approximately equal intensity (± 10%) separated by 1 GHz.

In some experiments single mode operation is desirable because of interference when a second mode optically pumps another absorption transition. Single mode operation is accomplished with a second solid etalon 15 mm thick (FSR 7 GHz), with 20% reflectivity on both sides. The output is 50 mW, stable to ± 100 MHz and ± 20% in amplitude, with 2 W of 514.5 nm pump. The spectral bandwidth is less than 10 MHz FWHM.

B. Production of BaO and Observation of Photoluminescence

The experimental arrangement used for observing microwave optical double resonance is shown in Fig. 4. The vacuum system is assembled from commercial 10 cm i.d. stainless steel sections with simple O-ring and clamp interconnections.[21]

Dye laser light, focused to a beam diameter less than 1 mm enters the photoluminescence region from the top through a Brewster angle window and a 3 mm aperture. Barium metal is vaporized from an alumina crucible in a tungsten basket heater. Barium vapor is entrained in argon and carried into the photoluminescence region where it reacts with oxygen.[21] Microwave radiation is introduced

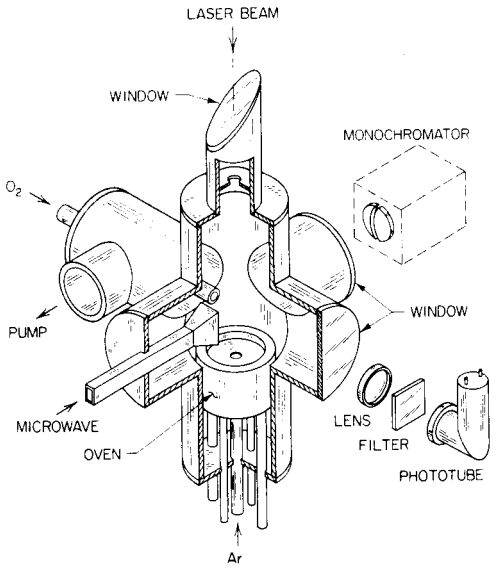

FIG. 4. The photoluminescence region in the MODR experiment. Dye laser radiation passes through the Brewster window and into the oven. Photoluminescence is observed as a vertical column of light, 1 cm in front of the microwave horn. Laser light is polarized along the microwave propagation direction and the microwave E vector is in the horizontal plane.

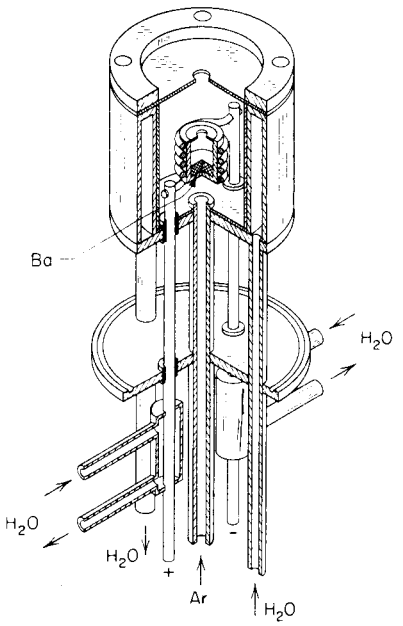

FIG. 5. Barium oven. Electrical connections to the tungsten basket heater are water-cooled, copper-jacketed (not shown) stainless steel rods. The crucible is surrounded by a tantalum-lined, water-cooled copper heat shield. The heat shield is electrically insulated from the heater electrodes by boron nitride spacers.

into the photoluminescence region by a horn radiator. Photoluminescence is monitored by side window photomultipliers with S-5 spectral response. One photomultiplier views the output of a 3/4 meter double monochromator (dispersion 0.54 nm/mm at 600 nm) and another photomultiplier monitors the photoluminescence through a short wavelength cutoff filter and a 20 nm FWHM interference filter.

The barium oven is shown in Fig. 5. A basket-shaped tungsten heater is used which consists of three strands of 1 mm diameter wire. Approximately 20 g of Ba is placed in a 5 cm^3 alumina crucible covered by a tantalum cap with a 3 mm aperture. Typically the oven is heated by 55 A at 5.5 V (ac) and the temperature inside the crucible is 1000 °K.[21] Under these operating conditions, one charge of barium lasts 10 h or more. The crucible is suspended inside a water-cooled, tantalum-lined copper chamber. Argon flows into this chamber at 1 cm^3/sec STP and sweeps barium vapor into the photoluminescence region through a 6 mm aperture in a 0.1 mm thick tantalum baffle. Normal operating pressure in the photoluminescence region is 0.2 torr. A flow of 0.01 cm^3/sec STP of oxygen is injected 6 cm from the photoluminescence region. In the photoluminescence region, the partial pressure of $^{138}Ba^{16}O$ $X\,^1\Sigma$ $(v=0)$ is $\sim 10^{-4}$ torr.[7b] A 7 liter/sec mechanical vacuum pump is used.

Before beginning a search for a double resonance transition, it is necessary to select a microwave transition between a specific pair of rotational levels. In this work the choice of microwave transitions was limited to rotational levels below $J=6$, since microwave oscillators above 77 GHz were unavailable. Suppose, for example, that a double resonance transition between electronically excited rotational levels $J'=2$ and $J'=3$ is chosen. Then for a specific $A\,^1\Sigma$–$X\,^1\Sigma$ vibrational band, there are four transitions by which either $J'=2$ or $J'=3$ can be optically pumped. Two of these are R-branch $(J''\rightarrow J'=J''+1)$ transitions, $R(1)$ and $R(2)$, and two are P-branch $(J''\rightarrow J'=J''-1)$ transitions, $P(3)$ and $P(4)$. If either $R(1)$ or $P(3)$ is optically pumped, $J'=2$ is populated and the microwave absorption $J'=2\rightarrow 3$ transition will be observable. If either $R(2)$ or $P(4)$ is optically pumped, $J'=3$ is populated and the microwave stimulated emission $J'=3\rightarrow 2$ transition will be observable. If for example one wishes to observe the $J''=2\rightarrow 3$ transition in the ground state, one of the $R(2)$, $P(2)$, $R(3)$, or $P(3)$ lines would be optically pumped.

Tuning the dye laser to one of four usable transitions is not a trivial matter. There are two distinct problems: how to determine which vibrational and rotational molecular transition the dye laser is pumping, and then how to tune the laser systematically to pump one of the four useful rotational transitions.

C. Assigning the Photoluminescence–Optical Spectroscopy

Dye laser-induced photoluminescence is observed in which BaO molecules are optically pumped out of the first eight vibrational levels $(v''=0-7)$ of the $X\,^1\Sigma$ electronic ground state. Photoluminescence involving rotational levels from $J=0$ to $J\sim 100$ and from the two most abundant isotopic species $^{138}Ba^{16}O$ (70%) and $^{137}Ba^{16}O$ (12%) is observed.

If the laser pumps the $X\,^1\Sigma$ $(v'', J'')\rightarrow A\,^1\Sigma$ (v', J') transition, the photoluminescence will consist of transitions from $A\,^1\Sigma$ $(v', J')\rightarrow X\,^1\Sigma$ (many v'', $J''=J'\pm 1$). The photoluminescence spectrum will appear as a progression of doublets. The energy splitting between members of a doublet is $B_v''(4J'+2)$. Thus, if B_v'' is known, and it is possible to measure the doublet splitting with an accuracy of $\pm 2B_v''(0.6\ cm^{-1}\approx 0.02$ nm), it is possible to determine J'. Successive doublets will be separated by vibrational intervals of the $X\,^1\Sigma$ state and (Franck–Condon factors permitting) the shortest wavelength doublet will be near the position of the $A\,^1\Sigma$ (v')–$X\,^1\Sigma$ $(v''=0)$ bandhead.[22] For BaO A–X,

the position of the shortest wavelength doublet and the wavelength of the laser line determine the vibrational quantum numbers of the optically-pumped transition.

Once v' and J' are known, it is also useful to know if the laser is pumping the $P(J'+1)$ transition ($J''=J'+1$) or the $R(J'-1)$ transition ($J''=J'-1$). If the photoluminescence doublet at the wavelength of the dye laser line is scanned, the transition which coincides with the laser line will appear more intense due to nonresonantly scattered laser light. The $P(J'+1)$ line is always at longer wavelength than the $R(J'-1)$ line. In this work all microwave transitions are observed when the laser pumps a P-branch transition.

Due to the small size of isotopic shifts in BaO, it is not possible to establish, by the optical spectroscopic means at our disposal, which BaO isotopic species is being optically pumped. However, since microwave spectra for the $X\,^1\Sigma$ state of $^{138}Ba^{16}O$, $^{137}Ba^{16}O$, $^{136}Ba^{16}O$, and $^{135}Ba^{16}O$ are known,[23] it was possible to identify the isotopic species being pumped by a double resonance experiment. The laser was tuned to the $P(3)$ line of the $A-X$ (3, 1) band. The $^{138}Ba^{16}O\,X\,^1\Sigma$ ($v''=1$, $J''=2\rightarrow 3$) transition was observed at 55.855 GHz and then, without changing the wavelength of the laser, the $A\,^1\Sigma$ ($v'=3$, $J'=2\rightarrow 3$) transition was observed at 45.740 GHz.

D. Tuning the Dye Laser to a Specific Molecular Line

When solid intracavity etalons are used to stabilize a dye laser, tuning the laser frequency is necessarily discontinuous and often requires a complex iterative sequence of adjustments of the tuning mirror and two etalons. With a single 1.5 mm thick etalon in the laser cavity, it is not possible to tune the laser more than 0.05 nm without adjusting the tuning mirror. However, it is possible following the procedure described below to tune the laser to pump any BaO transition between 570–600 nm.

The laser is tuned with the return mirror (M_1 of Fig. 3) to within 0.05 nm of the calculated position of the desired transition by measuring the laser wavelength with a calibrated monochromator. Insertion of a 1.5 mm thick etalon into the dye laser cavity causes the laser to oscillate in two modes separated by 1 GHz. Tilting the etalon perpendicular to the plane of dispersion tunes the laser in 90 MHz jumps, the longitudinal mode separation of the laser cavity. The laser is tuned to the nearest BaO transition by observing photoluminescence either by eye or with a photomultiplier–filter combination. The optically pumped transition is then assigned from the measured $P-R$ spacing as described in Sec. III. C. The *calculated* wavelength of the transition being pumped is compared with the *calculated* wavelength of the desired transition. If the transition being pumped by the laser is more than 0.05 nm from the desired transition, the laser is tuned in 0.1 nm steps (the free spectral range of the 1.5 mm etalon) by adjusting the tuning mirror. If the laser is within 0.05 nm of the desired line, it is often possible to tune the laser to the line by tilting the 1.5 mm intracavity etalon. Once the desired line is found, a 15 mm thick etalon also is inserted in the cavity to obtain single mode operation. In this configuration the laser will usually continue to pump the desired transition for several hours with occasional adjustments. It is convenient to monitor the spectral purity and stability of the dye laser with three extracavity etalons: a 3 GHz free spectral range spectrum analyzer and two solid etalons with free spectral ranges of 200 and 20 GHz.

E. Microwave Spectroscopy

50 to 500 mW of microwave radiation at frequencies between 12 and 77 GHz is generated by various oil-bath-cooled klystrons. Microwave radiation enters the photoluminescence region from a rectangular horn radiator. Neither microwave resonant cavities nor lenses to focus the microwave radiation are employed, nor is any attempt made to measure absorption of microwave radiation. Microwave transitions are observed and the frequencies are measured in two ways. When searching for a new microwave transition, microwave frequency is repetitively swept over a 100 MHz interval by applying a voltage ramp to the klystron reflector. The sweep rate is typically 50 MHz/msec. The frequency at any point in the sweep is measured by beating the klystron against a phase-locked, frequency-counted, 4–8 GHz oscillator. Sweep voltage for the klystron is generated by a 100 channel signal averager. Input to the signal averager is the 1 MΩ terminated output of the monochromator (1.1 nm bandpass)–photomultiplier. Typically the double resonance signal appears with $S/N>10$ after about 2 min of signal averaging. The signal FWHM, broadened by klystron frequency drift, is typically 15–20 MHz.

Once a transition is found it is often possible to obtain a slightly more accurate measure of its frequency using phase sensitive detection. The microwave radiation is amplitude modulated (on–off ratio > 10 dB) at 100 Hz by a ferrite switch. The klystron is phase locked by a continuously tunable frequency stabilizer which is capable of being voltage tuned by 0.1%. A frequency-counted 4–8 GHz oscillator is phase locked to the

klystron. The frequency of the klystron is swept 50 MHz in lock at 5 MHz/min. Observed linewidths are 10–15 MHz FWHM. Narrower (2–6 MHz) linewidths were observed in previously reported Ar^+ laser MODR experiments with BaO.[7] A radiative lifetime of 300 nsec corresponds to a radiative linewidth of 0.5 MHz. At this time the dependenceof MODR lineshapes on pressure, laser power, and microwave power are not understood.

Typically the double resonance signal for transitions in the $X\,^1\Sigma$ state is 5% of the total photoluminescence and 2% for transitions in the $A\,^1\Sigma$ state. The sensitivity of MODR experiments reported here is limited by noise of a nonstatistical nature which seems to constitute a fixed percentage of the photoluminescence (0.2% with 1 sec time constant). For microwave transitions in the $A\,^1\Sigma$ state, the double resonance signal is proportional to microwave power. Saturation of the MODR signal at high microwave power is observed for microwave transitions in the $X\,^1\Sigma$ state. Double resonance signal strength ΔI varies nonlinearly with laser power, but the percentage increase in photoluminscence intensity at microwave resonance, $\Delta I/I$, is independent of laser power. Photoluminescence intensity I varies nonlinearly with laser power; a decrease in single mode laser power from 50 mW to 5 mW results in a less than sixfold decrease in photoluminescence. Focussing the laser has not observably altered $\Delta I/I$.

IV. RESULTS

A. Microwave Spectra of BaO $X\,^1\Sigma$ and $A\,^1\Sigma$

Rotational transition frequencies and resultant rotational constants for the BaO $X\,^1\Sigma$ and $A\,^1\Sigma$ states measured in this work are listed in Table I. Rotational constants are calculated from observed microwave transition frequencies and previously reported centrifugal distortion constants for the $A\,^1\Sigma$ ($D = 8.4$ kHz)[12] and $X\,^1\Sigma$ ($D = 8.165$ kHz)[12] states. For the $J-1-J$ transition

$$\nu = 2BJ - 4DJ^3 \tag{28}$$

Microwave transitions in $A\,^1\Sigma$ ($v = 2$–5) and in $X\,^1\Sigma$ ($v = 1$) are observable because BaO $X\,^1\Sigma$ molecules are continuously produced in the photoluminescence region with significant populations of vibrationally-excited states. The occurrence of significant populations of vibrationally-excited molecules considerably extends the number of MODR transitions accessible within the limited tuning range of available dye lasers. Molecules in vibrational levels as high as $X\,^1\Sigma$ ($v = 7$) have been optically pumped thereby exciting photoluminescence from levels as high as $A\,^1\Sigma$ ($v = 9$). Although quantitative measurements have not been made, the population of $X\,^1\Sigma$ ($v = 7$) is no more than a factor of 100 smaller than the population of $X\,^1\Sigma$ ($v = 0$). Listed in Table II are the $A-X$ vibrational bands that were optically pumped while the various

TABLE I. Observed MODR transition in BaO $X\,^1\Sigma$ and $A\,^1\Sigma$.

Electronic state	v	Transition $J \leftrightarrow J+1$	Measured frequency (MHz)	B_v(MHz)[a,c]
$X\,^1\Sigma$	0	0–1	18702.(1)[d]	
		1–2	37404.(1)	
		2–3	56106.(1)	9351.1
	1	2–3	55855.(2)	9309.3
$A\,^1\Sigma$	0	2–3	46376.(2)	7729.5
	1	1–2	30760.5(1.0)	
		2–3	46142.(1)	7690.3
	$^{137}Ba^{16}O$	2–3	46177.7(1)	7696.4
	2	2–3	45986.(1)	7664.5
	3	1–2	30493.(2)	
		2–3	45740.(1)	
		3–4	60984.5(1.5)	
		4–5	76226.8(1.5)	7623.3
	4	2–3	45551.(1)	7592.0
	5	2–3	45397.3(1.0)	7566.4
	7	1–2	29927.6[b]	
		2–3	44891.4[b]	7482.0

[a] Uncertainty in each B_v is ±0.3 MHz.
[b] From Ref. 7.
[c] Corrected for centrifugal distortion; D ($X\,^1\Sigma$) = 8.165 kHz, D ($A\,^1\Sigma$) = 8.4 kHz.
[d] Uncertainties in ( ) are two standard deviations.

TABLE II. $A-X$ bands pumped for observed MODR transitions.

Microwave transitions observed	Optically-pumped BaO $A\,^1\Sigma - X\,^1\Sigma$ band	Laser λ (nm)
$X\,^1\Sigma$ $v=0$	1–0	580.8
	7–0	496.5[a]
$v=1$	3–1	570.3
$A\,^1\Sigma$ $v=0$	0–0	598.1
$v=1$	1–0	580.8
$v=2$	2–1	586.7
$v=3$	3–1	570.3
$v=4$	4–2	576.1
$v=5$	5–3	581.9
$v=7$	7–0	496.5[a]

[a] Ar^+ laser line.

microwave transitions were observed.

Although the $X\,^1\Sigma$ state is free of perturbations, the $A\,^1\Sigma$ state is known to be extensively perturbed by four states or substates designated X, Y, Z, and Q.[12,13] The effect of these perturbations, shown in Fig. 6, is evident in the failure of the measured rotational constants to be fit smoothly by the functional form $B(v) = B_e - \alpha_e(v+\frac{1}{2})$. Also shown in Fig. 6 are rotational constants which are adjusted to compensate for the largest perturbation of each $A\,^1\Sigma$ level, that due to the Y state. The corrected rotational constant is

$$B_{\text{corr}} = B_{\text{obs}} + [H_{AY}^2(B_A - B_Y)]/(E_A - E_Y)^2 \,. \qquad (29)$$

H_{AY} is the interaction between the A and Y states measured by Lagerqvist *et al.*[12] The corrected rotational constants show significantly less scatter than the observed constants. For $v=1$ and 3 significant perturbation effects, due to perturbations by the Z state, still remain. The $B(v)$ function obtained from a least squares fit to the corrected rotational constants is

$$B(v) = 0.25832(2) - 0.001070(5)\,(v+\tfrac{1}{2})\ \text{cm}^{-1}. \qquad (30)$$

It is not possible to correct the previously reported rotational constant for $A\,^1\Sigma$ ($v=7$) which is seriously affected by perturbations by the X and Y states.

Kovacs and Lagerqvist[13] predict a perturbation in $A\,^1\Sigma$ ($v=3$) near $J=5$ and 6 by the Q state. In an attempt to observe this perturbation the $J=1 \rightarrow 2$, $2 \rightarrow 3$, $3 \rightarrow 4$, and $4 \rightarrow 5$ transition frequencies were measured and no trace was found of a perturbation, which would appear as a discontinuity in the rotational energy. However, if the predicted energy of the Q state is in error by as little as ± 2 cm^{-1}, the point of maximum perturbation would occur at either $J<0$ or $J>7$ and no discontinuity in the rotational energy would have been observed. Additional discussion of the BaO perturbations and related perturbations in CaO and SrO will appear elsewhere.[24] The observed and corrected rotational constants for $A\,^1\Sigma$ are compared with the constants reported by Lagerqvist *et al.*[12] in Table III. All rotational constants measured in this work agree with the optical spectroscopic constants obtained by Lagerqvist *et al.*[12] within the stated optical error limits. Error limits for the MODR rotational constants are 10 times smaller than the optical limits. Perturbation effects become considerably more visible with the higher precision of MODR spectroscopy.

TABLE III. Comparison of observed and corrected $A\,^1\Sigma$ rotational constants (in cm^{-1}).

$A\,^1\Sigma$ v	B_{obs}	B_{corr}	B_{optical}[a]
0	0.25783(1)[c]	0.25783	0.2578(1)
1	0.25652(1)	0.25667	0.2564(2)
2	0.25566(1)	0.25567	0.2556(2)
3	0.24529(1)	0.25450	0.2541(2)
4	0.25324(1)	0.25353	0.2532(2)
5	0.25239(1)	0.25246	0.2523(2)
7	0.24957(1)	...	...
B_e	0.25841(2)	0.25832(2)[b]	0.2583(2)
α_e	0.001151(3)	0.001070(5)[b]	0.00113(7)

[a] From Ref. 12.
[b] Recommended constants for BaO $A\,^1\Sigma$.
[c] Uncertainties in ( ) correspond to two standard deviations.

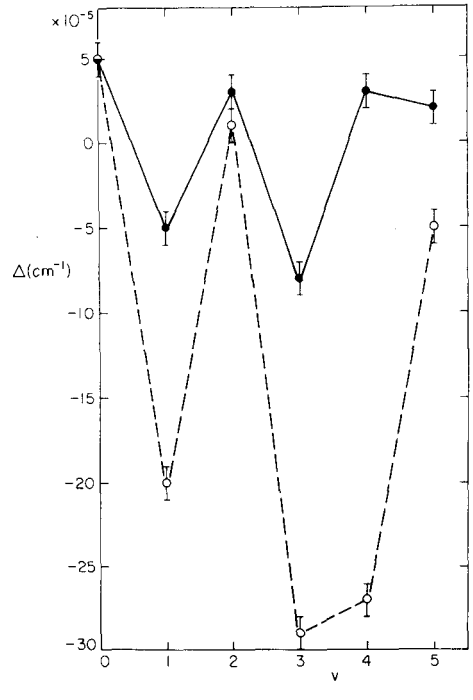

FIG. 6. Scatter in BaO $A\,^1\Sigma$ rotational constants due to perturbations. $\Delta = B_v - 0.25832 + 0.00107\,(v+\frac{1}{2})$ is plotted vs v for both observed (○) and corrected (●) rotational constants. Error bars correspond to two standard deviations. Dotted and solid lines, respectively, connect the points corresponding to observed and corrected rotational constants.

The observed $J=2 \rightarrow 3$ transition in $^{137}Ba^{16}O$ $A^1\Sigma$ $(v=1)$ cannot be used to obtain a hyperfine eq_0Q constant. The ratio of the corresponding $^{138}Ba^{16}O$ and $^{137}Ba^{16}O$ transition frequencies is, within experimental error, equal to the ratio of the reduced masses. Even if there were a residual isotope shift not accounted for by the change in reduced mass, perturbation effects could be considerably larger than any expected hyperfine shift.

Initial attempts to measure electric dipole moments by MODR Stark effects have been frustrated by electrical breakdown at electric field strengths less than 200 V/cm.

B. Test of MODR Models

Three experimental observations show that optical pumping of BaO $A-X$ transitions by a single frequency, 50 mW, cw dye laser is near the strong optical pumping limit. Photoluminescence intensity varies nonlinearly with laser power. MODR transitions in BaO $X\,^1\Sigma$ are observed with $\Delta I/I = 5\%$, which is considerably larger than the predicted 0.2% effect [Eq. (2)] for the weak optical pumping limit. The large observed MODR signal implies that the dye laser depletes level 1 $(n_1 < n_1^0)$ by pumping molecules out of level 1 faster than thermalizing collisions can replenish them. MODR transitions $J \rightarrow J+1$ and $J \rightarrow J-1$ in BaO $A\,^1\Sigma$ are always observed to correspond to an increase in total photoluminescence intensity. An increase in total photoluminescence intensity implies an increase in optical pumping rate. An excited state microwave transition increases the optical pumping rate $(n_3 - n_1)S$ by decreasing n_1.

The transition dipole model for excited state MODR is supported by a sequence of three observations of BaO $A\,^1\Sigma$ $(v=1)$ $J'=2 \rightarrow 3$ transitions under various optical pumping and detection polarization conditions. In these experiments the microwave electric field is Z directed and the microwaves and detected photoluminescence propagate in the X direction. First $J'=2$ was populated by optically pumping a $P(3)$ transition. The laser was polarized perpendicular (X polarized) to the microwave electric field, a polarization predicted by the transition dipole model to optimize the MODR effect. For the $J=2 \rightarrow 3$ transition, an increase in Z-polarized photoluminescence is predicted, accompanied by a smaller decrease in X or Y polarized photoluminescence. Observed $\Delta I/I$ was $+5.1 \pm 0.5\%$ for Z-polarized photoluminescence and $+3.3 \pm 0.3\%$ for Y polarization. The polarization dependent MODR effect is superimposed on a polarization independent strong (nonlinear) optical pumping MODR effect. Next, with a Z-polarized dye laser, observed $\Delta I/I$ is $3.5 \pm 0.6\%$ for Z-polarized photoluminescence and $2.7 \pm 0.6\%$ for Y polarization. Thus the predicted decrease in $\Delta I/I$ is observed when the optical pump polarization is not optimal for populating $|M| = J$ sublevels. Finally, the X-polarized dye laser was tuned to pump the $P(4)$ line and the $J=3 \rightarrow 2$ transition was observed. The transition dipole model predicts a decrease in Z- and an increase in Y-polarized photoluminescence. $\Delta I/I$ was $+2.5 \pm 0.3\%$ for Z and $+5.0 \pm 0.8\%$ for Y polarization, exactly the expected opposite of the observed $\Delta I/I$'s for the $J=2 \rightarrow 3$ transition.

Near the strong optical pumping limit, $\Delta I/I$ is expected and observed to be nearly independent of laser power [Eqs. (18) and (24)] and to vary linearly with microwave power [Eqs. (21) and (27)]. The critical parameters in the three level steady state model are $\frac{1}{2}\tau_g \tau X^2$ (or $\frac{1}{2}\tau_e \tau X^2$) and $S_m \tau_g$ (or $S_m \tau_e$). These saturation parameters should have values near 1 when $\Delta I/I$ no longer increases linearly with laser or microwave power.

$\frac{1}{2}\tau_g \tau X^2$ can be estimated using Eq. (17) with $\omega = \omega_{31}$, $\tau_e = \tau_g = \tau$, and $S_m = 0$. The observed sixfold decrease in photoluminescence when dye laser power was reduced from 50 to 5 mW is predicted if $\frac{1}{2}\tau\tau_g X^2 = 1.5$ at 50 mW.

The saturation parameters $\frac{1}{2}\tau_g \tau X^2$ and $S_m \tau_g$ may be calculated from known electric dipole transition moments, estimated microwave and laser power densities, and relaxation rates estimated from MODR linewidths. Let

$$\tau_g = \tau_e = \tau_m = \tau,$$

$$(2\pi\tau)^{-1} = 10 \text{ MHz},$$

where 10 MHz is the FWHM of observed MODR lines. The squared transition moment matrix element for a $(J,\ M=0) \rightarrow (J+1,\ M=0)$ microwave or optical transition is

$$|\langle J, 0 | \mu | J+1, 0 \rangle|^2 = \mu^2 (J+1)^2/(2J+1)(2J+3) \approx \mu^2/4. \tag{31}$$

The dipole moment for BaO $X\,^1\Sigma$ is 8 D[25] and the microwave electric field which corresponds to a power density of 100 mW/cm^2 is 8.7 V/cm; thus when $\omega_m = \omega_{12}$

$$S_m \tau_g = \tfrac{1}{2}\tau_g \tau_m X_m^2 = 1.4 \quad .$$

This value of $S_m \tau_g$ indicates that microwave transitions in BaO $X\,^1\Sigma$ are near saturation. In BaO $X\,^1\Sigma$ MODR experiments the onset of saturation of $\Delta I/I$ and microwave power broadening was observed. The absence of microwave saturation effects in BaO $A\,^1\Sigma$ MODR indicates that the electric dipole moment of $A\,^1\Sigma$ is smaller than 8 D.

The transition moment for the BaO $A\,^1\Sigma - X\,^1\Sigma$ (1, 0) band (corresponding to $R_e = 1.76$ D[21] and a Franck–Condon factor [26] of 0.042) is 0.36 D. The

optical electric field which corresponds to 100 mW uniformly distributed over a 1 mm diameter beam is 98 V/cm. Thus

$$\tfrac{1}{2}\tau_g \tau X^2 = 0.36.$$

This value is too small to account for observed laser saturation of I and of $\Delta I/I$. However, the optical saturation parameter $\frac{1}{2}\tau_g \tau X^2$ is considerably underestimated by neglecting the Gaussian profile of the laser beam (see Sec. V).

V. REQUIREMENTS FOR MODR

Microwave optical double resonance effects have been shown to be observable in the weak optical pumping limit. Somewhat larger MODR signals, particularly for ground state MODR, occur near the strong optical pumping limit. Four factors determine whether the strong optical pumping limit is attainable: optical electric field strength, relaxation rates, the electronic transition moment, and the Franck–Condon factor of the optically-pumped transition.

The optical electric field as a function of distance X from the center of a Gaussian profile laser beam is

$$E(X) = E \sin\omega t \exp[-X^2/W^2], \tag{32a}$$

$$E = 21.9 I_0^{1/2}/W \text{ (volts/centimeter)}. \tag{32b}$$

W is the radius (centimeter) at which the laser power is $1/e^2$ times its maximum and I_0 is the laser power (watts). Beams of radius $2W$, W, $0.5W$, and $0.1W$ contain respectively 99.97%, 87.5%, 39.3%, and 2% of the total power of the laser. A 100 mW laser with $W = 0.2$ mm has an optical electric field $E > 270$ V/cm for $X < 0.1$ mm. $E = 270$ V/cm is a good upper limit for the optical electric field available with a 100 mW dye laser.

Nonequilibrium populations established by optical and microwave pumping are relaxed by several processes. Molecules diffuse into and out of the laser beam. For a beam with $W = 0.2$ mm the transit relaxation time is $\tau_{\text{transit}} \approx 10^{-6}$ sec. Rotational relaxation, typically 10 MHz/torr, corresponds to $\tau_{\text{pressure}} \approx 10^{-7}$ sec at 0.2 torr. Electronically-excited states decay radiatively usually with $\tau_{\text{rad}} > 5 \times 10^{-9}$ sec. Lower limit values for τ_g and τ_e are

$$\tau_g = [(1/\tau_{\text{transit}}) + (1/\tau_{\text{pressure}})]^{-1} \cong 10^{-7} \text{ sec},$$

$$\tau_e = [(1/\tau_{\text{transit}}) + (1/\tau_{\text{pressure}}) + (1/\tau_{\text{rad}})]^{-1} \cong 5 \times 10^{-9} \text{ sec}.$$

Note that $\tau_e \leq \tau_g$. τ and τ_m, which appear in Eqs. (12) and (13), can be smaller than τ_e or τ_g near the strong microwave and optical limits, but this effect will be neglected.

For a $^1\Sigma - {}^1\Sigma$ transition in which the electronic transition moment R_e (Debyes) is independent of r-centroid

$$f_{v'v''} = 4.7 \times 10^{-7} q_{v'v''} \nu_{v'v''} R_e^2. \tag{33}$$

$f_{v'v''}$ is the oscillator strength, $q_{v'v''}$ is a Franck–Condon factor, and $\nu_{v'v''}$ is the frequency (cm^{-1}) of the transition. The transition dipole μ for the $(J, M = 0) \rightarrow (J \pm 1, M = 0)$ transition is related to the electronic transition moment:

$$\mu^2 \cong q_{v'v''} R_e^2/4. \tag{34}$$

If the lifetime of an excited electronic state is determined entirely by radiation to the electronic ground state, there is a relationship between the radiative lifetime and R_e:

$$1/\tau_{v'} = 3.14 \times 10^{-7} R_e^2 \sum_{v''} q_{v'v''} \nu_{v'v''}^3$$

$$\approx 3.14 \times 10^{-7} \nu_{v'0}^3 R_e^2. \tag{35}$$

Note that the quantity $\tau_{v'} \mu^2$ is independent of radiative lifetime and transition moment:

$$\tau_{v'} \mu^2 \approx 8.0 \times 10^5 q_{v'v''} \nu_{v'0}^{-3}. \tag{36}$$

For ground state MODR the optical saturation parameter is

$$\tfrac{1}{2}\tau_g \tau_e X^2 = 4.0 \times 10^{18} \tau_g E^2 q_{v'v''} \nu_{v'0}^{-3} \tag{37}$$

If $\tau_g = 10^{-7}$ sec, $E = 270$ V/cm, and $\nu = 17000$ cm^{-1}, the optical saturation parameter is

$$\tfrac{1}{2}\tau_g \tau_e X^2 = 6 \times 10^3 q_{v'v''}. \tag{38a}$$

Thus even for a Franck–Condon factor less than 1×10^{-3}, it should be possible to observe ground state MODR in the strong optical pumping limit. For excited state MODR, the optical saturation parameter is, if $\tau_e = 5 \times 10^{-9}$ sec,

$$\tfrac{1}{2}\tau_e^2 X^2 = 30 q_{v'v''}. \tag{38b}$$

Thus, even for transitions with a Franck–Condon factor as small as 0.03 and with a radiative lifetime as short as 5×10^{-9} sec, the strong optical pumping limit should be attainable.

In order to observe MODR transitions, it is desirable to operate near the strong microwave limit because the MODR signal $\Delta I/I$ increases linearly with microwave power until the microwave saturation parameter is near 1. For ground state MODR, the microwave saturation parameter is

$$\tfrac{1}{2}\tau_g^2 X_m^2 \cong 1.3 \times 10^{12} \mu^2 \tau_g^2 E^2, \tag{39}$$

where μ is the permanent electric dipole moment in Debyes. If $\tau_g = 10^{-7}$ sec and $\mu = 1$ D, a microwave electric field of 9 V/cm is required for saturation. This corresponds to an easily attainable power density of 100 mW/cm^2. For excited state MODR, the microwave saturation parameter is $\frac{1}{2}\tau_e^2 X_m^2$. If $\tau_e = 5 \times 10^{-9}$ sec, the microwave electric

field required for saturation is 175 V/cm or a power density of 41 W/cm^2. This is a high power density, but still easily attainable in a resonant microwave cavity.

ACKNOWLEDGMENTS

The skillful and rapid fabrication of numerous parts needed for this work in the Physics Department Machine Shop and particularly the craftsmanship of Howard Nickel are gratefully acknowledged. This work would not have been possible without the enthusiastic support of Professor H. W. Lewis. Professor H. P. Broida has been more than generous with advice, penetrating criticism, and much needed equipment.

*This research was supported by Army Grant No. DA-ARO-D-31-124-72-G181, NSF Grant No. GP-35672X, and AFOSR Grant No. AFOSR-70-1851.

†Visiting Scientist from the Department of Chemistry, Faculty of Science, Kyushu University, Fukuoka, Japan.

‡On leave from the National Bureau of Standards, Boulder, CO 80302.

[1]S. J. Silvers, T. H. Bergeman, and W. Klemperer, J. Chem. Phys. **52,** 4385 (1970).

[2]K. German and R. N. Zare, Phys. Rev. Lett. **23,** 1207 (1969).

[3]R. W. Field and T. H. Bergeman, J. Chem. Phys. **54,** 2936 (1971).

[4]A. M. Ronn and D. R. Lide, Jr., J. Chem. Phys. **47,** 3669 (1967); T. Shimizu and T. Oka, Phys. Rev. A **2,** 1177 (1970).

[5]S. M. Freund and T. Oka, Appl. Phys. Lett. **21,** 60 (1972).

[6]R. Solarz and D. H. Levy, J. Chem. Phys. **58,** 4026 (1973).

[7](a) R. W. Field, R. S. Bradford, D. O. Harris, and H. P. Broida, J. Chem. Phys. **56,** 4712 (1972). (b) R. W. Field, R. S. Bradford, H. P. Broida, and D. O. Harris, J. Chem. Phys. **57,** 2209 (1972).

[8]T. W. Hänsch, I. Shahin, and A. L. Schawlow, Phys. Rev. Lett. **27,** 707 (1971).

[9]C. G. Stevens, M. W. Swagel, R. Wallace, and R. N. Zare, Chem. Phys. Lett. **18,** 465 (1973).

[10](a) W. Hartig and H. Walther, Appl. Phys. **1,** 171 (1973). (b) R. L. Barger, M. S. Sorem, and J. L. Hall, Appl. Phys. Lett. **22,** 573 (1973).

[11]R. E. Drullinger and R. N. Zare, J. Chem. Phys. **51,** 5532 (1969); J. Chem. Phys. (to be published).

[12]A. Lagerqvist, E. Lind, and R. F. Barrow, Proc. Phys. Soc. Lond. A **63,** 1132 (1950).

[13]I. Kovács and A. Lagerqvist, Ark. Fys. **2,** 411 (1950).

[14]K. Evenson, J. Dunn, and H. P. Broida, Phys. Rev. **136,** A1566 (1964).

[15]R. S. Freund and T. A. Miller, J. Chem. Phys. **56,** 2211 (1972).

[16]C. B. Harris, J. Chem. Phys. **54,** 972 (1971).

[17]M. Takami and K. Shimoda, Jap. J. Appl. Phys. **11,** 1648 (1972).

[18]A. Dienes, E. P. Ippen, and C. V. Shank, IEEE J. Quantum Electron. **QE-8,** 388 (1972).

[19]H. W. Kogelnik, E. P. Ippen, A. Dienes, and C. V. Shank, IEEE J. Quantum Electron. **QE-8,** 373 (1972).

[20]M. Hercher and H. A. Pike, Opt. Commun. **3,** 65 (1971).

[21]S. E. Johnson, J. Chem. Phys. **56,** 149 (1972) and S. E. Johnson, Ph.D. thesis, University of California, Santa Barbara, CA, 1972.

[22]P. C. Mahanti, Proc. Phys. Soc. Lond. **46,** 51 (1934).

[23]J. Hoeft, F. J. Lovas, E. Tiemann, and T. Törring, Z. Naturforsch. A **25,** 1750 (1970).

[24]R. W. Field (unpublished).

[25]L. Wharton, M. Kauffman, and W. Klemperer, J. Chem. Phys. **37,** 621 (1962).

[26]T. Wentink, Jr. and R. J. Spindler, Jr., J. Quant. Spectrosc. Radiat. Transfer **12,** 129 (1972).